Medium-spin γ-ray spectroscopy of the transitional nucleus ^{160}Er

K. Dusling,[1] N. Pietralla,[1] G. Rainovski,[1] T. Ahn,[1] B. Bochev,[1] A. Costin,[1]
T. Koike,[1] T. C. Li,[1] A. Linnemann,[2] S. Pontillo,[1] and C. Vaman[1]
[1]*Department of Physics & Astronomy, State University of New York, Stony Brook, New York 11794-3800, USA*
[2]*Institut für Kernphysik, Universität zu Köln, D-50937 Köln, Germany*
(Received 6 August 2005; published 31 January 2006)

The nucleus ^{160}Er, with the structural parameter $R_{4/2} = E(4_1^+)/E(2_1^+) = 3.10$, falls on the transition path between the critical point of the vibrator-rotor shape phase transition and the rigid rotor limit, thus serving as a critical test of the CBS rotor model, which describes this transition region. Medium-spin states of ^{160}Er have been populated via the reaction ^{159}Tb(^{6}Li,5n) and new levels have been identified and interpreted as the even-spin members of the γ band and members of the β vibrational band. Level energies and branching ratios are compared to the CBS rotor model predictions.

DOI: 10.1103/PhysRevC.73.014317 PACS number(s): 21.10.Re, 21.60.Ev, 23.20.En, 27.70.+q

I. INTRODUCTION

Shape phase transitions in atomic nuclei have been used as testing grounds for nuclear models for many years and recently have gained much attention owing to the analytic solutions of the Bohr Hamiltonian presented by Iachello [1–3]. The solution of interest to this report is X(5) [2], which describes a situation close to the shape phase transition from spherical vibrator ($R_{4/2} = 2.0$) to rigid rotor ($R_{4/2} = 3.33$). X(5) now serves as a benchmark in nuclear structure and empirical examples have already been found (e.g., ^{152}Sm [4] and ^{150}Nd [5]).

A recently developed generalization of the X(5) solution, the confined β-soft (CBS) rotor model [6], describes all nuclei on the transition path between the X(5) critical point and the rigid-rotor limit by parametrizing the width of a square-well potential in the deformation variable β.

The CBS rotor model (see [6] for details of the derivation) is an approximate analytical solution to the Bohr Hamiltonian in the quadrupole shape parameters β and γ under the assumption of a separable potential of the form $V(\beta,\gamma) = v(\beta) + u(\gamma)$. For sufficiently axially symmetric prolate nuclei one might consider a steep harmonic oscillator in γ (as is done in Refs. [2, 7]) with $\gamma \approx 0^\circ$. By assuming a decoupling of the β and γ degrees of freedom the solution to the wave equation is of the form $\Psi(\beta,\gamma,\theta_i) = \xi_L(\beta)\eta_K(\gamma)\mathcal{D}^L_{M,K}(\theta_i)$, where $\mathcal{D}$ denotes the Wigner functions with θ_i being the Euler angles for the orientation of the intrinsic system, and $\eta_K(\gamma)$ is the appropriate wave function in γ. The "radial" differential equation as a function of the shape parameter β,

$$-\frac{\hbar^2}{2B}\left[\frac{1}{\beta^4}\frac{\partial}{\partial\beta}\beta^4\frac{\partial}{\partial\beta} - \frac{1}{3\beta^2}L(L+1) + u(\beta)\right]\xi_L(\beta) = E\,\xi_L(\beta), \tag{1}$$

contains the angular momentum dependence through the centrifugal term. The CBS rotor model assumes for prolate axially symmetric nuclides an infinite square-well potential, $u(\beta)$, with boundaries at $\beta_M > \beta_m \geqslant 0$. For this potential the wave equation is analytically solvable [6]. The ratio $r_\beta = \beta_m/\beta_M$ parameterizes the width of this potential, that is, the stiffness of the nucleus in the β degree of freedom. For $r_\beta = 0$ the X(5) limit is obtained with large fluctuations in β. The rigid-rotor limit without fluctuations in β corresponds to $r_\beta \to 1$.

The quantization condition of the CBS rotor model is

$$Q^{r_\beta}_{\nu(L)}(z) = J_{\nu(L)}(z)Y_{\nu(L)}(r_\beta z) - J_{\nu(L)}(r_\beta z)Y_{\nu(L)}(z) = 0, \tag{2}$$

with J_ν and Y_ν being Bessel functions of first and second kind of irrational order $\nu(L) = \sqrt{[L(L+1) - K^2]/3 + 9/4}$. For a given structural parameter r_β and any spin value L the sth zero of Eq. (2) is denoted by $z^{r_\beta}_{L,s}$. The full solution of Eq. (1) with the aforementioned choice of CBS square-well potentials is then given as

$$\xi_{L,s}(\beta) = c_{L,s}\,\beta^{-3/2}\left[J_\nu\left(z^{r_\beta}_{L,s}\frac{\beta}{\beta_M}\right) - \frac{J_\nu\left(r_\beta z^{r_\beta}_{L,s}\right)}{Y_\nu\left(r_\beta z^{r_\beta}_{L,s}\right)}Y_\nu\left(z^{r_\beta}_{L,s}\frac{\beta}{\beta_M}\right)\right], \tag{3}$$

with normalization

$$1/c^2_{L,s} = \int_{\beta_m}^{\beta_M}\beta^4[\xi_{L,s}(\beta)]^2 d\beta \tag{4}$$

and with the eigenvalues

$$E_{L,s} = \frac{\hbar^2}{2B\beta_M^2}\left(z^{r_\beta}_{L,s}\right)^2. \tag{5}$$

The $B(E2)$ values can be obtained from the matrix elements of the quadrupole operator

$$T^{E2} = e_{\text{eff}}\beta\left\{D^{(2)}_{\mu,0}(\Omega)\cos\gamma + \frac{1}{\sqrt{2}}\left[D^{(2)}_{\mu,2}(\Omega) + D^{(2)}_{\mu,-2}(\Omega)\right]\sin\gamma\right\}. \tag{6}$$

The CBS rotor model has already shown considerable success in describing both excited 0_2^+ (where the evolutionary trajectory of these 0_2^+ states as a function of $R_{4/2}$ is predicted [6]) and the ground bands of strongly deformed nuclei in both the rare earth and actinide region with an accuracy of order 10^{-3} [8]. ^{160}Er serves as a good test of the CBS rotor model as

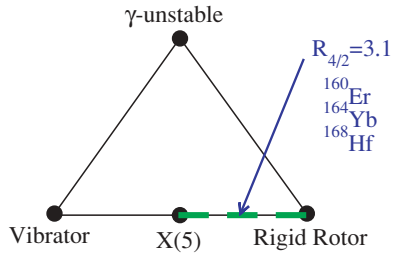

FIG. 1. (Color online) Schematic structural triangle for the nuclear collective model [9] where the vertices represent idealized limits of structure and the legs transition regions. The CBS model describes the transition region from X(5) to the symmetric rigid rotor (dashed line). Nuclides with $R_{4/2} = 3.1$ (e.g.,^{164}Yb, ^{168}Hf, and ^{160}Er, on which this paper focuses) might be intermediate between X(5) and the rigid rotor.

it may be a candidate for a nucleus falling on the transition path between X(5) and the rigid rotor. It has an $R_{4/2} = 3.1$ value that is expected for a situation between X(5) ($R_{4/2} = 2.9$) and the rigid rotor ($R_{4/2} = 3.33$) as is schematically emphasized in Fig. 1. Although transitional nuclei in this mass region have recently been discussed in the framework of the interacting boson model (IBM) [10], it will be interesting to compare both excitation energies and relative $B(E2)$ values found in this experiment to the predictions of the IBM and the CBS rotor model.

II. EXPERIMENT

Excited states in ^{160}Er have been populated via the ^{159}Tb(^{6}Li,5n) fusion-evaporation reaction at a beam energy of 52 MeV from the SUNY Stony Brook Tandem-LINAC facility. The experiment was performed at SUNY Stony Brook's Stony Cube setup [11]. Six HPGe detectors were positioned at polar angles of $\pm 45^\circ$, $\pm 135^\circ$, and $\pm 90^\circ$ relative to the beam direction, ideal for angular correlation measurements. A total of 9×10^8 $\gamma\gamma$-coincidence events were recorded during the course of the experiment.

Figure 2 shows the projection of the low-energy spectrum collected in coincidence over the course of the experiment. The known ground band transitions of ^{160}Er are labeled.

III. DATA ANALYSIS AND RESULTS

New excited states in ^{160}Er were identified using $\gamma\gamma$-coincidence relations. As an example of the procedure used Fig. 3 shows two spectra; the upper spectrum is in coincidence with the $6^+ \rightarrow 4^+$ (376-keV) ground band transition and the lower spectrum is in coincidence with the $8^+ \rightarrow 6^+$ (464-keV) ground band transition. In this figure the peaks of interest include the 1156-keV $\beta \rightarrow$ ground and the 1185-keV $\gamma \rightarrow$ ground transitions, which are only seen in coincidence with the $6^+ \rightarrow 4^+$ ground band transition, thus placing these two γ decays in the corresponding position in the level scheme as shown in Fig. 4. Other decay transitions as seen in the level scheme are labeled.

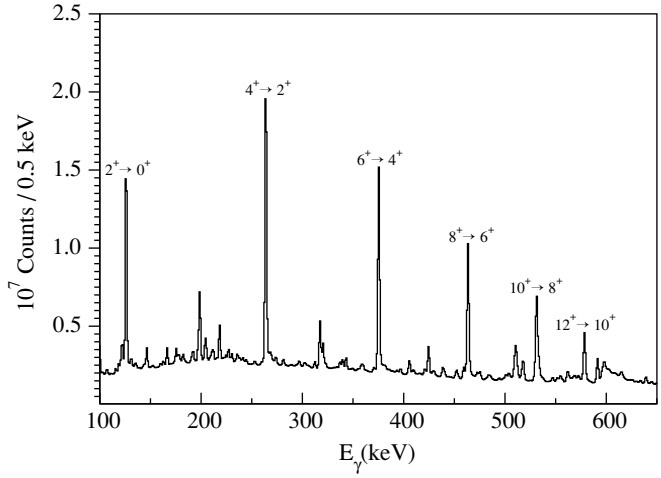

FIG. 2. $\gamma\gamma$-coincidence projection from the ^{159}Tb(^{6}Li,5n)^{160}Er experiment with the ground band transitions in ^{160}Er labeled.

The spin quantum number of excited states and the multipole mixing ratios of transitions were determined from $\gamma\gamma$ angular correlation measurements. The geometry of Stony Brook's spectrometer results in five $\gamma\gamma$ angular correlation groups, which are defined by three angles: $\theta_{1,2}$ given as the polar angle between the observed γ ray and the beam axis and ϕ defined as the angle between the planes intersecting the beam axis and an emitted γ ray.

Because this is the first time an experiment of this type has been performed on the Stony Cube at Stony Brook, we show an example of the angular correlation analysis of two transitions between levels of known spin and parity. Figure 5 shows the relative intensities of a known $12^+ \rightarrow 10^+$ stretched quadrupole transition and a known $11^- \rightarrow 10^+$ stretched dipole transition in coincidence with the $10^+ \rightarrow 8^+$ ground band transition. The solid curves show the predicted values [12] for the two transitions. The level of agreement is excellent

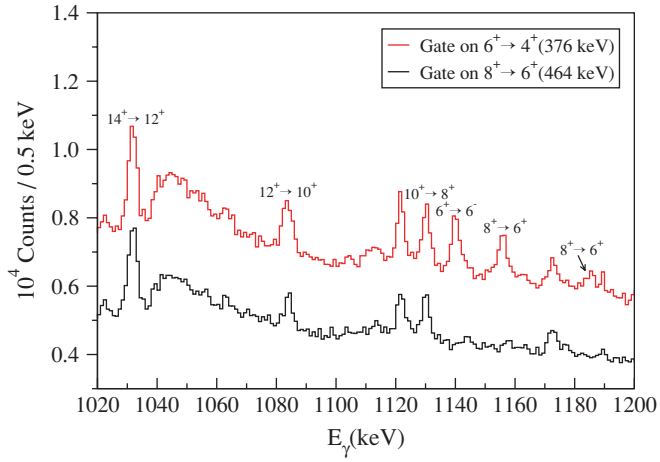

FIG. 3. (Color online) Coincidence relationship between the $6^+ \rightarrow 4^+$ (upper spectrum) and $8^+ \rightarrow 6^+$ (lower spectrum) ground band transitions showing the placement of the $8^+_\beta \rightarrow 6^+$ (1156-keV) and the $8^+_\gamma \rightarrow 6^+$ (1185-keV) transitions.

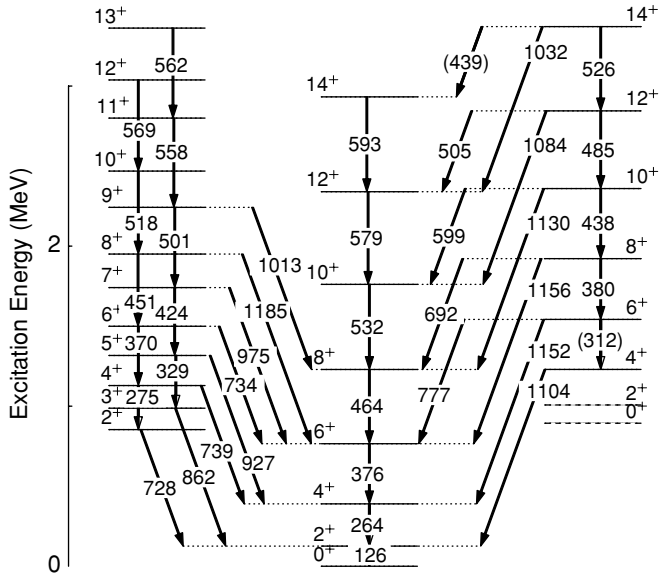

FIG. 4. Partial level scheme of ^{160}Er observed in this experiment. The observation of the 439- and 312-keV transitions (labels in parentheses) are uncertain owing to contaminants in the reaction. The dashed levels were not identified in this experiment but seen in prior β-decay experiments [13].

considering that there are no free parameters[1] other than an overall normalization.

[1]The magnetic substate distribution is assumed to be a Gaussian of width $\sigma(J)$ evaluated from an empirical relation of 16 known pure $E1$ and $E2$ transitions in the data. It has been checked that the conclusions drawn in the following stay the same within quoted uncertainties when the small uncertainties in $\sigma(J)$ are taken into account.

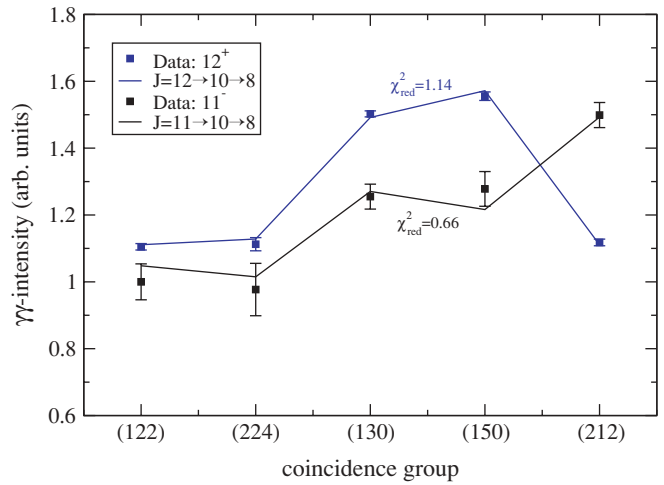

FIG. 5. (Color online) Angular correlation analysis of two known (pure $E2$ and pure $E1$) transitions showing the quality of data produced at SUNY Stony Brook's Stony Cube setup. The coincidence groups are labeled by three integers, which denote in units of $\pi/4$ the two angles between the observational directions and the beam and between the planes defined by the beam and the γ-decay directions.

TABLE I. Level and γ-ray energies, spin assignments, multipole mixing ratios, and intensity data for the transitions observed in ^{160}Er. The γ-ray energies are accurate to ± 0.5 keV. $I_\gamma^{\rm norm}$ refers to the intensity of the decay transition normalized to the $4_1^+ \rightarrow 2_1^+$ transition. (Errors are not given because the data were determined either from the total projection or from the efficiency-corrected gate on the $4_1^+ \rightarrow 2_1^+$ transition; thus the errors of the normalized intensities are much larger compared to the relative intensities given in the fifth column.) Energy levels marked with an *n* are newly identified states.

$E_{\rm Level}$	E_γ (keV)	$I_i^\pi \rightarrow I_f^\pi$	δ	$I_\gamma^{\rm rel}$	$I_\gamma^{\rm norm}$
125.8	125.8	$2^+ \rightarrow 0^+$		100	115
389.8	264.0	$4^+ \rightarrow 2^+$		100	100
765.5	375.7	$6^+ \rightarrow 4^+$		100	92
1229.3	463.9	$8^+ \rightarrow 6^+$		100	73
1761.0	531.6	$10^+ \rightarrow 8^+$		100	66
2339.9	578.9	$12^+ \rightarrow 10^+$		100	33
2931.8	591.9	$14^+ \rightarrow 12^+$		100	14
3122.7	782.8	$14^+ \rightarrow 12^+$		100	4
1229.6	1103.9	$4^+ \rightarrow 2^+$		100	<1
1542.1^n	1152.3	$6^+ \rightarrow 4^+$		100(17)	2
	(312.3)	$6^+ \rightarrow 4^+$		24(7)	
	776.8	$6^+ \rightarrow 6^+$		<2	
1921.8^n	1156.3	$8^+ \rightarrow 6^+$		100(5)	2
	379.3	$8^+ \rightarrow 6^+$		53(2)	
	692.4	$8^+ \rightarrow 8^+$		19(2)	
2359.6^n	1130.3	$10^+ \rightarrow 8^+$		100(14)	2
	437.7	$10^+ \rightarrow 8^+$		77(18)	
	599.6	$10^+ \rightarrow 10^+$		98(32)	
2844.6^n	1083.6	$12^+ \rightarrow 10^+$		100(12)	2
	485.3	$12^+ \rightarrow 10^+$		80(10)	
	505.7	$12^+ \rightarrow 12^+$		28(10)	
3371.4^n	1031.5	$14^+ \rightarrow 12^+$		100(28)	3
	526	$14^+ \rightarrow 12^+$		9(2)	
	(439)	$14^+ \rightarrow 14^+$		<45	
853.7	727.9	$2^+ \rightarrow 2^+$		100	1
987.4	861.4	$3^+ \rightarrow 2^+$		100	<1
1128.9	739.1	$4^+ \rightarrow 4^+$	-7^{+3}_{-17}	100(6)	10
	(274.1)	$4^+ \rightarrow 2^+$		11(3)	
1316.8	927.0	$5^+ \rightarrow 4^+$	$-5.5^{+0.9}_{-1.2}$	100(4)	6
	329.4	$5^+ \rightarrow 3^+$		24(3)	
1499.3^n	733.8	$6^+ \rightarrow 6^+$	$-8.2^{+2.3}_{-5.6}$	100(8)	7
	370.4	$6^+ \rightarrow 4^+$		31(5)	
1740.9	975.4	$7^+ \rightarrow 6^+$	$-2.11^{+0.26}_{-0.29}$	100(7)	6
	424.1	$7^+ \rightarrow 5^+$		71(7)	
1950.4^n	1184.9	$8^+ \rightarrow 6^+$		71(7)	
	451.1	$8^+ \rightarrow 6^+$		100(15)	2
2242.2	1013.4	$9^+ \rightarrow 8^+$		46(6)	
	501.3	$9^+ \rightarrow 7^+$		100(5)	4
2468.8^n	518.4	$10^+ \rightarrow 8^+$		100	
2799.8	557.6	$11^+ \rightarrow 9^+$		100	
3038.2^n	569.4	$12^+ \rightarrow 10^+$		100	
3362.1	562.3	$13^+ \rightarrow 11^+$		100	

Nine new levels and 22 new γ-ray lines have been placed in the level scheme. All of the information obtained in this experiment is summarized in Table I. A total of eleven γ-decay branching ratios and four multipole mixing ratios have been measured.

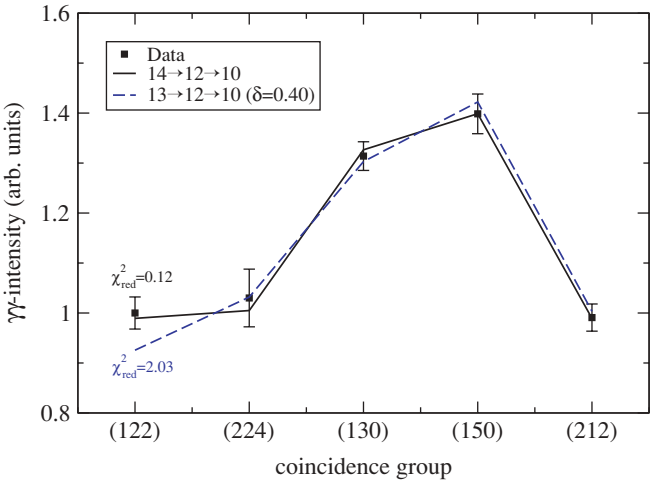

FIG. 6. (Color online) Assignment of spin quantum number $J = 14$ for the 3373.5-keV level from the $\gamma\gamma$ angular correlation analysis. The solid squares show the relative intensities of the 1031.5-keV γ ray in coincidence with a member of the ground band. All of the $\gamma\gamma$ coincidences between the 1031.5-keV transition and any member of the ground band were summed to reduce the background. The multipole mixing ratio δ was treated as a free parameter in the case of the $J = 13$ hypothesis.

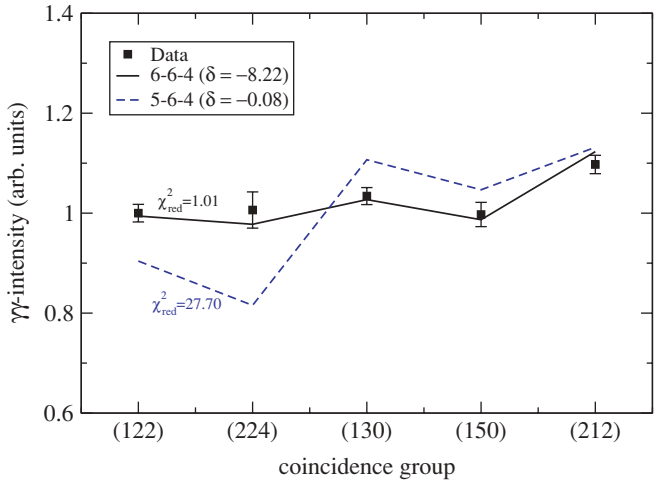

FIG. 7. (Color online) Measurement of spin quantum number $J = 6$ for the 1499.3-keV level from the $\gamma\gamma$ angular correlation analysis. Also shown for comparison is the simulation for a $J = 5$ hypothesis. In both cases the multipole mixing ratio δ was treated as a free parameter.

Figure 4 shows the partial level scheme of ^{160}Er with all of the new levels and γ rays seen in this experiment. The new findings of this report include the identification of the $K = 0$ band and the finding of the even-spin members of the γ band. (Previously, only the 0^+ and 2^+ states of the $K = 0$ band were known and only the $2+$ as well as the odd-spin members to $J = 13^+$ of the γ band were known [14].)

We focus first on the excited $K = 0$ band (the rightmost band in Fig. 4) where we have identified five new levels. The strongest evidence for the spin and parity assignments is the 14^+ spin assignment, made from the correlation results, to the uppermost member of this band. Figure 6 shows the relative intensity of the $14^+ \rightarrow 12^+$, $K = 0 \rightarrow$ ground band transition in coincidence with the ground band for each correlation group. The high statistics obtained, by summing the spectra in coincidence with the $8^+ \rightarrow 6^+$, $6^+ \rightarrow 4^+$, or $4^+ \rightarrow 2^+$ ground band transitions, suggests a spin assignment of 14^+ to this level of the $K = 0$ band. This is seen in Fig. 6, where the solid curve corresponds to a theoretical $14^+ \rightarrow 12^+ \rightarrow 10^+$ (with both transitions pure $E2$) and the dashed curve corresponds to the theoretical $13^+ \rightarrow 12^+ \rightarrow 10^+$ with a pure $E2$ $12^+ \rightarrow 10^+$ transition after a preceding $E2/M1$ mixed (least-squares fit, $\delta = +0.40$) $13^+ \rightarrow 12^+$ transition. It is seen that the best fit is obtained for the 14^+ simulation, whereas group (122) deviates by more than 2σ for the 13^+ simulation. It should be noted that the fit for the 14^+ assignment has one less degree of freedom and yet better agreement with the data [$\chi^2_{red}(J = 14) = 0.12$ versus $\chi^2_{red}(J = 13) = 2.03$], quantitively supporting this conclusion. The spin assignments of the remaining levels in the $K = 0$ band are consistent with the angular correlation analysis; however, these assignments are ambiguous since the possibility of an odd spin assignment (where the transition is a mixed $E2/M1$) cannot be ruled out; that is, a mixing ratio can always be found to fit the data within the uncertainties. (It should be mentioned that these mixing ratios suggest a large dipole component, which is unreasonable for quadrupole collective structures.) The convincing 14^+ assignment in addition to the agreement with the spin assignments in the remaining levels leads us to conclude the reasonable interpretation that this structure is a $\Delta J = 2$ sequence of even-spin positive-parity states. The transitions from the lowest two levels of the $K = 0$ band were not observed in this experiment but are known from prior β-decay experiments [13]. Comparison with the normalized intensity of the $4^+_\beta \rightarrow 2^+$ transition shows that we do not expect to see the $4^+_\beta \rightarrow 2^+_\beta$ 222.0-keV transition in our data because the expected intensity ratio as given from CBS model predictions [$I_{CBS}(4^+_\beta \rightarrow 2^+_\beta)/I_{CBS}(4^+_\beta \rightarrow 2^+_1] = 0.04$] shows that the 222.0-keV transition would be below our detection limit. The reasonable assignment of $K = 0$ to the new band structure is strongly supported by the systematics of neighboring Er isotopes to be discussed later.

We now focus on the $K = 2$ band (the leftmost band in Fig. 4). The spin quantum numbers were measured in the same fashion as described earlier and multipole mixing ratios were extracted via a χ^2 minimization procedure. As an example Fig. 7 shows the relative intensity of the 734-keV $6^+ \rightarrow 6^+_1$ transition in coincidence with the ground band for each correlation group. The solid curve shows a simulation for a mixed $E2/M1$ $6 \rightarrow 6 \rightarrow 4$ cascade, where the multipole mixing ratio in the upper half of the cascade was treated as a free parameter. For comparison the simulation for a mixed $E2/M1$ $5 \rightarrow 6 \rightarrow 4$ cascade, again with δ treated as a free parameter, is shown by the dashed curve. From the figure it is seen that an unambiguous spin assignment of $J = 6$, with an almost pure $6^+ \rightarrow 6^+ E2$ transition, can be made for this level.

IV. DISCUSSION

The main results of this experiment include the finding of two collective quadrupole structures, the first intrinsic $K = 0$

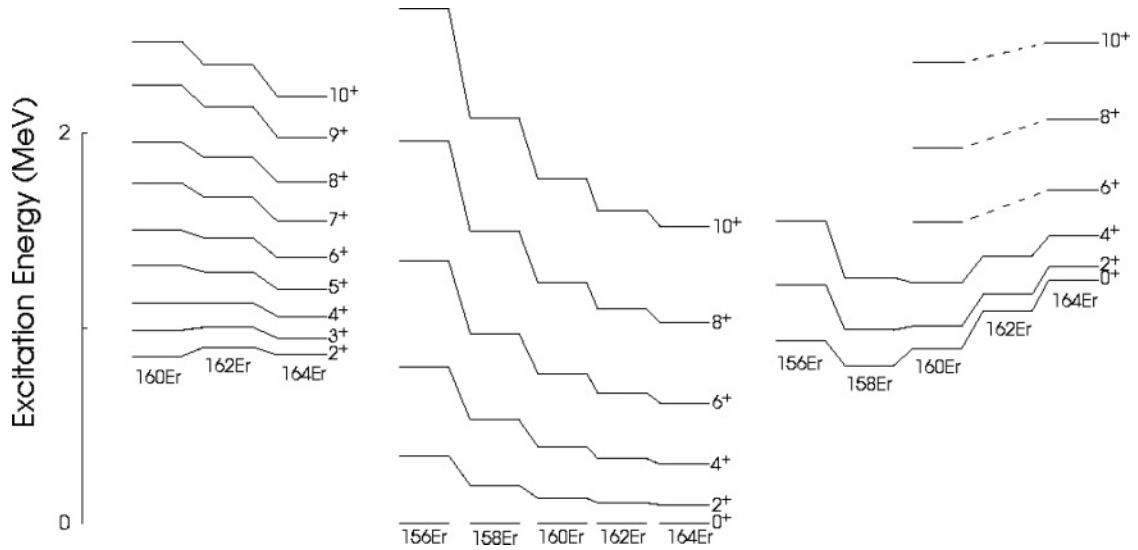

FIG. 8. Systematics of γ, yrast, and β bands (left to right) of erbium isotopes showing the smooth variation in energy levels of the newly found excited states in ^{160}Er as a function of neutron number. Data for neighboring isotopes are taken from [15].

band, which we identify as a quasi β vibrational band, as well as the even members of a $K = 2$ band, which we identify as the missing even-spin members of the already identified γ vibrational band [14]. We show a comparison of the low-lying level scheme of ^{160}Er with its neighboring isotopes in Fig. 8 for all of the known quadrupole collective structures. It is seen that the excitation energies of the excited levels vary smoothly as a function of neutron number for the ground band and the γ and β vibrational bands. These regularities further support our assignments of the newly found levels in ^{160}Er.

Eleven γ-intensity branching ratios and four multipole mixing ratios have been measured, many for the first time, and it is interesting to compare these findings to the CBS model predictions. By a fit to the ground band (up to spin 12_1^+ to remain below any backbending) the values $r_\beta = 0.204$ and $\hbar^2/2B\beta_M^2 = 125.8$ keV were found and then used to make parameter-free predictions of the energies [and thus moment of inertia (MoI)] and γ-decay branching ratios of the β vibrational band. In addition, parameter-free predictions, except for scale, for the energies and branching ratios for the γ band were also made.

The underlying mechanism behind the CBS model is the centrifugal stretching of the nucleus [i.e., increase in $\langle\beta\rangle(J)$ as a function of spin], which can be classically understood as an increase in the MoI with spin. In Fig. 9 the evolution of the MoI with spin, here plotted as the relative dynamical moment of inertia defined as

$$\frac{\theta_K(J)}{\theta_K(K+2)} \equiv \left[\frac{J(J+1)-K(K+1)}{4K+6}\right] \times \frac{E(J=K+2)-E(K)}{E(J)-E(K)}, \qquad (7)$$

is compared to the CBS rotor model predictions. The upper graph in Fig. 9 shows good agreement between the CBS prediction and experiment. The middle graph shows the parameter-free prediction of the evolution of the relative MoI for the β vibrational band. Here we chose to plot $\theta(J)/\theta(6)$ instead of the usual $\theta(J)/\theta(2)$ since the $6_\beta^+ \rightarrow 4_\beta^+$ is the lowest transition in the band that was observed in this experiment. Overall the agreement is good even though deviations are seen at $J = 0$ and $J = 2$. This is due to an increase in energy

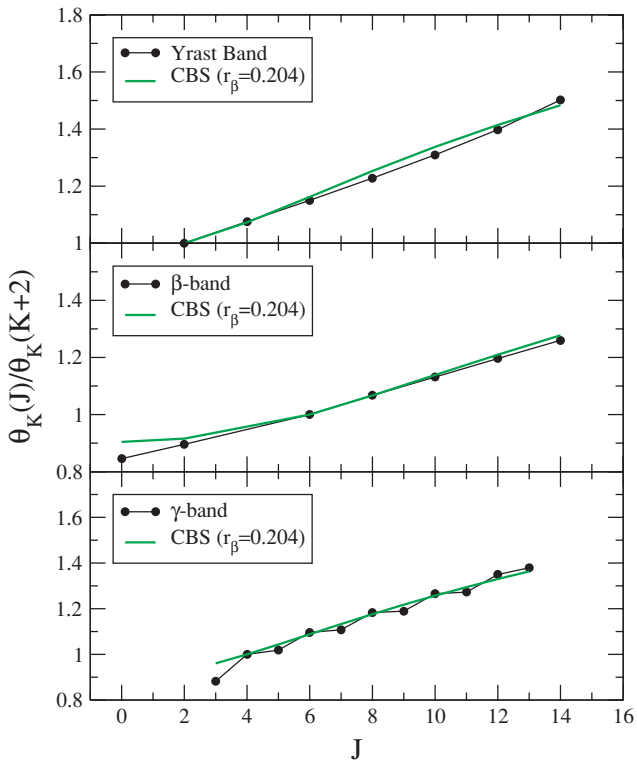

FIG. 9. (Color online) Evolution of the relative moment of inertia $[\theta_K(J)/\theta_K(K+2)$ as defined in Eq. (7)] as a function of spin for the ground band (upper graph) β vibrational band (center graph) and γ vibrational band (lower graph) with the CBS rotor model predictions (solid curve). The curve in middle graph is normalized to the lowest transition observed in our data [i.e., $\theta_0(J)/\theta_0(6)$ is what is plotted].

of the first excited 0^+ state, which is not described by the model. The reason for this is not understood but may be due to the wave function's sensitivity to the details of the potential in β. Since the 0_2^+ sits lowest in this potential it would be affected the most by any small deviations from the schematic square-well potential used in the CBS model. It should also be mentioned that when parameter-free predictions of the absolute energies of the β band are made, much larger deviations are seen (e.g., the absolute excitation energy of the first excited 0^+ state [6] is overpredicted by $\approx$10%). Moreover, the energy scale of excited states within the β band is overpredicted by the CBS rotor model. This is to be expected since the intrinsic excitation might change the internal structure, which is not accounted for in this model. We should also mention that the same problem persists in the X(5) solution as well [4,5,16–18] and seems to be a general problem of collective models [19].

The lower graph shows the evolution of the MoI in the γ band as a function of spin. The overall agreement is good but one immediately notices the staggering of even/odd spin level energies that occurs, which is observed in many transitional nuclei and is still not fully understood quantitatively. Level energy staggering in the γ vibrational band of deformed nuclei has been attributed earlier to band mixing (see, e.g. [20] for a case in the Er isotopic sequence) or to deviation from axial symmetry [21, 22 and references therein]. Let us discuss the staggering observed in the γ band of ^{160}Er in more detail. In the absence of any perturbation we expect both the even and odd members of the γ band to follow the same energy formula, that is, the MoI should be a smoothly varying function of spin. One might expect that a two-state mixing scenario with either the β band or ground-state band could account for this staggering, but both of these possibilities can be ruled out. Since there are no low-lying positive-parity odd-spin structures observed in this nucleus, we expect that the odd-spin members of the γ band are at the true, or unperturbed, energies. Therefore the unperturbed even-spin states of the γ band can be interpolated from the odd-spin states. (In this paper we take these energies from the CBS rotor model predictions.) In the case of band mixing between the γ band and the ground-state band all even-spin states of the former would be shifted to higher energies, thereby decreasing the energy difference $E(J = \text{odd}) - E(K)$ to the $K^\pi = 2^+$ band head relative to the unperturbed situation. This energy difference appears in the denominator of Eq. (7) and would result in an increase of the relative MoI for odd-J states, which contrasts with the data in Fig. 9. Another possibility could be band mixing with the nearby $K = 0$ band. However, two-state band mixing with the $K = 0$ band is ruled out as well, owing to the crossing in energies after spin 6^+ in the β and γ bands. In a band-mixing scenario the sign of the staggering must switch at the crossing of the two bands. Instead, the observation is a smooth increase in the staggering regardless of the relative positions (above or below) of the close-lying even-spin states of the β band. We believe that the staggering is related to fluctuations about axial symmetry [22]. The effects of β-γ coupling in the presence of square-well potentials in β have recently been discussed by Caprio [23]. Our data on ^{160}Er might be considered as direct evidence for these coupling effects [23].

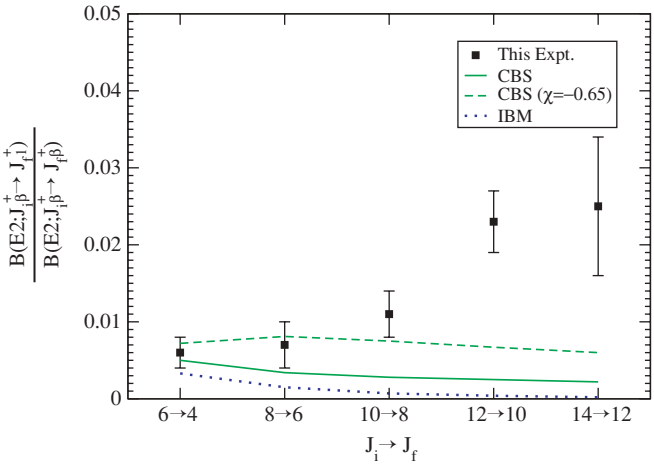

FIG. 10. (Color online) Measured interband to intraband branching ratios for transitions of known pure $E2$ character in the β band. IBM predictions (parameters for ^{160}Er taken from [10]) are given by the dotted blue curve. The solid green curve shows the CBS rotor model's predictions. The dashed green curve shows the CBS model's predictions with inclusion of a higher order term in β for the $E2$ operator with expansion parameter χ [see Ref. [6] for the definition of $T(E2)$ to second order], which was found from a fit to the known absolute $B(E2)$ values [25] in the ground band. Therefore, we should stress that both curves are parameter-free predictions of these branching ratios.

It is seen that the CBS rotor model has considerable success in describing the relative energy levels of all the low-lying quadrupole collective structures in ^{160}Er with the largest inconsistencies being the incorrect scale in the prediction of the energy levels in the β band and in the staggering that occurs in the γ band. We stress that a one-parameter fit to the observed centrifugal stretching of the ground-state band leads, within the framework of the CBS rotor model, to a reliable prediction of the centrifugal stretching for collective intrinsic excitations.

It is also interesting to compare the prediction of branching ratios with those found in this experiment. Intraband versus interband branching ratios are particularly interesting because their absolute sizes are not predicted by the rigid-rotor model. In Table II the energy-reduced γ-intensity branching ratios [relative $B(E2)$ values in the case of stretched quadrupole transitions] are compared to those of the CBS rotor model. In addition the X(5), relative rigid-rotor, and IBM (parameters for ^{160}Er taken from [10]) values are shown for comparison. In the X(5) and CBS models the β band to ground-state band $E2$ transitions are related to the softness of the potential in β and can be obtained in a parameter-free way. In the rigid-rotor model interband transitions are caused by intrinsic transition matrix elements that depend on the deformation parameters of the bands. For the convenient discussion of the interband to intraband $E2$ branching ratios we define the parameters $M_\gamma = 100(\langle\gamma|E2|g\rangle/\langle\gamma|E2|\gamma\rangle)^2$ and $M_\beta = 100(\langle\beta|E2|g\rangle/\langle\beta|E2|\beta\rangle)^2$ as squares of relative intrinsic $E2$ matrix elements. Similarly, in X(5) and CBS one needs a corresponding parameter for the γ to ground-state band

TABLE II. Energy-reduced relative γ-decay intensities [relative $B(E2)$ values in the case of stretched quadrupole transitions] for the observed levels of the γ band and β band with the predictions made by X(5), the CBS rotor model, and the rigid-rotor model. Upper limits are given in the case of an unknown $M1$ admixture ($\leqslant$) or contamination ($<$).

$I_i \rightarrow I_f$	^{160}Er	X(5)	CBS	IBM	Rotor
			β band		
$14^+_\beta \rightarrow 12^+_\beta$	100	100	100	100	100
$\rightarrow 12^+$	2.5(9)	0.22	0.22	0.02	$1M_\beta$
$\rightarrow 14^+$	$<$31.9	1.21	1.21	0.06	$0.72M_\beta$
$12^+_\beta \rightarrow 10^+_\beta$	100	100	100	100	100
$\rightarrow 10^+$	2.3(4)	0.25	0.25	0.04	$1M_\beta$
$\rightarrow 12^+$	$\leqslant$29.0	1.47	1.47	0.08	$0.73M_\beta$
$10^+_\beta \rightarrow 8^+_\beta$	100	100	100	100	100
$\rightarrow 8^+$	1.1(3)	0.28	0.28	0.07	$1M_\beta$
$\rightarrow 10^+$	$\leqslant$26.3	1.85	1.85	0.09	$0.74M_\beta$
$8^+_\beta \rightarrow 6^+_\beta$	100	100	100	100	100
$\rightarrow 6^+$	0.7(3)	0.33	0.34	0.15	$1M_\beta$
$\rightarrow 8^+$	$\leqslant$1.8	2.42	2.38	0.09	$0.77M_\beta$
$6^+_\beta \rightarrow 4^+_\beta$	100	100	100	100	100
$\rightarrow 4^+$	0.6(2)	0.44	0.50	0.33	$1M_\beta$
$\rightarrow 6^+$	$<$0.09	3.35	3.16	0.08	$0.81M_\beta$
[a]$4^+_\beta \rightarrow 2^+$	100	100	100	100	100
$\rightarrow 4^+$	$\leqslant$35.6	635.7	397.0	3.1	90.9
[a]$2^+_\beta \rightarrow 4^+$	100	100	100	100	100
$\rightarrow 2^+$	$\leqslant$25.9	22.75	24.79	2.53	55.53
$\rightarrow 0^+$	14(3)	6.02	9.47	17.52	38.83
			γ band		
$9^+_\gamma \rightarrow 7^+_\gamma$	100	100	100	100	100
$\rightarrow 8^+$	$\leqslant$2.87	1.00N	1.00N	0.97	$0.97M_\gamma$
$8^+_\gamma \rightarrow 6^+_\gamma$	100	100	100	100	100
$\rightarrow 6^+$	$\leqslant$0.6	0.32N	0.31N	0.001	$0.31M_\gamma$
$7^+_\gamma \rightarrow 5^+_\gamma$	100	100	100	100	100
$\rightarrow 6^+$	1.8(2)	1.19N	1.19N	1.81	$1.14M_\gamma$
$6^+_\gamma \rightarrow 4^+_\gamma$	100	100	100	100	100
$\rightarrow 6^+$	10(2)	1.68N	1.67N	13.93	$1.54M_\gamma$
$5^+_\gamma \rightarrow 3^+_\gamma$	100	100	100	100	100
$\rightarrow 4^+$	2.3(3)	1.79N	1.76N	4.42	$1.67M_\gamma$
$4^+_\gamma \rightarrow 2^+_\gamma$	100	100	100	100	100
$\rightarrow 4^+$	7(2)	3.3N	3.2N	26.87	$2.94M_\gamma$

[a]Data taken from prior β-decay experiment [13]. It should be noted that because of the unobservable intraband transitions from the 4^+_β and 2^+_β states, the corresponding branching ratios are normalized to the interband transitions that are expected to be weak ($\approx$1 W.u.) where accurate qualitative predictions with a collective model are difficult.

transition matrix element, $N \equiv (\langle\gamma|E2|g\rangle/\langle\gamma|E2|\gamma\rangle)^2$ [7,24], which is related to the depth of the assumed potential of the γ degree of freedom in X(5) and the CBS rotor model and hence cannot be predicted by the model.

Interband to intraband $E2$ branching ratios for the γ band are shown at the bottom of Table II. The CBS model agrees with the data for the 7^+_γ, 5^+_γ, and 4^+_γ states within a factor of about 2. A larger deviation is seen only for the 6^+_γ state. The experimental limits on the branching ratios of the 9^+_γ and 8^+_γ states are in agreement with the CBS scheme as well. The IBM reproduces the data on the γ-band branching ratios remarkably well with the largest deviation for the 4^+_γ.

The interband to intraband $E2$ branching ratios from the β band are predicted by X(5), the CBS rotor model, and the IBM without any scaling parameter. The CBS model predicts the $J_\beta \rightarrow (J-2)_g$ branching ratios for the 6^+_β and 8^+_β within about the error bars. However, with increasing spin, deviations are seen in the band. This and the systematic underprediction of the data by the IBM is shown in Fig. 10.

V. SUMMARY

In summary, nine new levels in ^{160}Er have been identified with eight branching ratios and four multipole mixing ratios being measured for the first time. Both level energies and branching ratios [relative $B(E2)$ values] have been compared to the recently proposed confined β-soft rotor model with success. Quantitative agreement is seen between level energies in the ground and γ vibrational bands. The quality of agreement between the data on $E2$ branching ratios for the low-lying quadrupole collective structures and the CBS rotor model is discussed. The fact that the CBS model is able to quantitatively predict the evolution of the relative moment of inertia as well as make parameter-free predictions of the interband to intraband branching ratios in the β band is in itself an achievement, considering the difficulty [26] that still remains in fully understanding these structures.

ACKNOWLEDGMENTS

We would like to thank B. Gutschow, A. Lipski, and R. Lefferts for preparation of the beam and target. We are grateful to M. Caprio, R. F. Casten, I. Hamamoto, and P. von Brentano for useful discussions. This work is supported by NSF Grant No. PHY 0245018 and by DOE Grant No. DE-FG02-04ER41334.

[1] F. Iachello, Phys. Rev. Lett. **85**, 3580 (2000).
[2] F. Iachello, Phys. Rev. Lett. **87**, 052502 (2001).
[3] F. Iachello, Phys. Rev. Lett. **91**, 132502 (2003).
[4] R. F. Casten and N. V. Zamfir, Phys. Rev. Lett. **87**, 052503 (2001).
[5] R. Krücken, B. Albanna, C. Bialik, R. F. Casten, J. R. Cooper, A. Dewald, N. V. Zamfir, C. J. Barton, C. W. Beausang, M. A. Caprio, A. A. Hecht, T. Klug, J. R. Novak, N. Pietralla, and P. von Brentano, Phys. Rev. Lett. **88**, 232501 (2002).
[6] N. Pietralla and O. M. Gorbachenko, Phys. Rev. C **70**, 011304(R) (2004).
[7] R. Bijker, R. F. Casten, N. V. Zamfir, and E. A. McCutchan, Phys. Rev. C **68**, 064304 (2003).
[8] K. Dusling and N. Pietralla, Phys. Rev. C **72**, 011303(R) (2005).

[9] R. F. Casten, *Nuclear Structure from a Simple Perspective* (Oxford University Press, New York, 2000).
[10] E. A. McCutchan, N. V. Zamfir, and R. F. Casten, Phys. Rev. C **69**, 064306 (2004).
[11] R. M. Wirowski, dissertation, University of Cologne, 1993.
[12] R. M. Steffen and R. M. Wheeler, Nucl. Data Tables **11**, 351 (1973).
[13] B. Singh, A. Kogan, and S. K. Mark, Phys. Rev. C **28**, 2118 (1983).
[14] J. Simpson, M. A. Riley, J. R. Cresswell, D. V. Elenkov, P. D. Forsyth, G. B. Hagemann, D. Howe, B. M. Nyako, S. Ogaza, J. C. Lisle, and J. F. Sharpey-Schafer, J. Phys. G **13**, 847 (1987).
[15] National Nuclear Data Center, Brookhaven National Laboratory, http://www.nndc.bnl.gov/ (2005).
[16] D. Tonev, A. Dewald, T. Klug, P. Petkov, J. Jolie, A. Fitzler, O. Möller, S. Heinze, P. von Brentano, and R. F. Casten, Phys. Rev. C **69**, 034334 (2004).
[17] R. M. Clark, M. Cromaz, M. A. Deleplanque, R. M. Diamond, P. Fallon, A. Görgen, I. Y. Lee, A. O. Macchiavelli, F. S. Stephens, and D. Ward, Phys. Rev. C **67**, 041302(R) (2003).
[18] R. F. Casten, N. V. Zamfir, and R. Krücken, Phys. Rev. C **68**, 059801 (2003).
[19] W. T. Chou, Gh. Cata-Danil, N. V. Zamfir, R. F. Casten, and N. Pietralla, Phys. Rev. C **64**, 057301 (2001).
[20] C. Y. Wu, D. Cline, M. W. Simon, R. Teng, K. Vetter, M. P. Carpenter, R. V. F. Janssens, and I. Wiedenhover, Phys. Rev. C **61**, 021305(R) (2000).
[21] A. S. Davydov and G. F. Filippov, Nucl. Phys. **8**, 237 (1958).
[22] N. V. Zamfir and R. F. Casten, Phys. Lett. **B260**, 265 (1991).
[23] M. A. Caprio, Phys. Rev. C **72**, 054323 (2005).
[24] C. Fransen, N. Pietralla, A. Linnemann, V. Werner, and R. Bijker, Phys. Rev. C **69**, 014313 (2004).
[25] B. Bochev, S. Iliev, R. Kalpakchieva, S. A. Karamyan, T. Kutsarova, E. Nadzhakov, and T. Venkova, Yad. Fiz. **30**, 593 (1979); Sov. J. Nucl. Phys. **30**, 305 (1979).
[26] P. E. Garrett, J. Phys. G **27**, R1 (2001).